Journal of Polymer Research (2019) 26: 200
https://doi.org/10.1007/s10965-019-1855-9

ORIGINAL PAPER

Preparation and characterization of PVA proton exchange membranes containing phosphonic acid groups for direct methanol fuel cell applications

Wang Zhiwei[1] · Zheng Hao[1] · Chen Qiang[1] · Zhang Sumei[1] · Yang Feng[1] · Kang Jian[1] · Chen Jinyao[1] · Cao Ya[1] · Xiang Ming[1]

Received: 7 March 2019 / Accepted: 11 July 2019 / Published online: 29 July 2019

Abstract

In this paper, 2-phosphonobutane-1,2,4-tricarboxylic acid (PBTCA), which is an organic phosphonic acids (OPA), is selected as the protic media to prepare phosphonated proton exchange membranes based on polyvinyl alcohol (PVA) by solution casting technique. The obtained PVA membranes were characterized using fourier transform infrared (FT-IR) spectroscopy, thermogravimetric analysis (TGA), and wide angle X-ray diffraction (WAXD). The proton conductivities and the methanol permeabilities through the membranes were investigated in terms of various OPA content. The proton conductivity of the PVA membrane measured at room temperature was close to that of the nafion-117 membrane measured under the same test conditions (1.02×10^{-3} S·cm^{-1}). But in the low relative humidity (50%), the proton conductivity of the phosphonic proton exchange membrane has a conductivity of up to 8.17×10^{-5} S·cm^{-1}, which was significantly higher than that of the sulfonate proton exchange membrane. The methanol permeabilities of the PVA membranes were in the range of 10^{-7} to 10^{-6} cm^2/s in the room temperature, depending on the OPD content. The thermal stability of the composite membrane was enhanced with incorporating of PBTCA by presenting high initial decomposition temperature.

Keywords Proton exchange membrane · Organic phosphonic acid · Polyvinyl alcohol · Fuel cell

Introduction

With the rapid development of the world economy, the demand for energy is also increasing rapidly. With energy shortage and environmental pollution becoming more and more serious, more and more countries urgently need to develop new energy sources [1–3]. Proton exchange membrane fuel cell (PEMFC) attracts more and more researchers' attention because of its excellent performance of high energy density, low temperature start-up, small volume and no noise [4, 5]. The limitations of fuel cells today largely depend on the performance and durability of the proton exchange membranes. The function of the proton exchange membranes is basically to efficiently conduct protons and separate the anode and the cathode sides [6]. The proton conducting membranes employed in the fuel cells are typically based on hydrated sulfonated polymers in their protonated form. Sulfonic acid, as a kind of strong acid, has prominent proton dissociation ability and high proton conduction ability under the condition of complete hydration. However, the binding proton ability of sulfonate is very weak and cannot be completely dissociated at low humidity and low temperature. On the other hand, the proton conduction process of sulfonic acid group is strongly dependent on the participation of water [7]. Those result in the decrease of its proton conductivity under high temperature and low humidity condition.

Perfluorosulfonic acid (PFSA) membranes, such as Nafion, are deemed as the state-of-art PEM material because of its excellent chemical, mechanical, and thermal stability, as well as its relatively high proton conductivity when fully hydrated [8–10]. However, chemical destruction and conductivity degradation of the Nafion membrane are frequently observed in fuels cells that have been operated for a long term. High methanol permeability and high production cost also limit its application and promotion. Therefore, it is urgent to develop a new proton exchange membrane with low price, low methanol permeability and no excessive dependence on water content [11–13]. Apart from sulfonate,

✉ Chen Jinyao
chenjy111@126.com

[1] State Key Laboratory of Polymer Materials Engineering, Polymer Research Institute of Sichuan University, Chengdu 610065, People's Republic of China

phosphate can also be used as a proton transfer site in proton exchange membranes. Phosphoric acid is amphoteric (acidic and basic) which can function as both a proton donor and a proton receptor. This property of phosphoric acid makes it possible to form a dynamic hydrogen bond network in the membrane, which is helpful to proton conductivity. At the same time, phosphoric acid has higher thermal stability and oxidation resistance than sulfonic acid. Phosphate group can dissociate itself even in the absence of water and the free energy barrier for proton transfer between phosphate groups is low. However, little effort has been geared toward the area of phosphonated membranes for fuel cells [14, 15].

Polyvinyl alcohol (PVA) was chosen as the main material of proton exchange membrane due to its splendid hydrophilicity and mechanical properties. There are a large number of hydroxyls in the molecular chain, giving rise to the easy formation of hydrogen bonds between molecules. Compared with Nafion membrane, PVA membrane can effectively reduce the methanol permeability, and the price is also very cheap. As a result, PVA membrane has been widely used in the preparation of proton exchange membrane [16, 17]. Meanwhile, butane phosphonate-1,2,4-tricarboxylic acid (PBTCA), a kind of poly-phosphatic hydrocarbon, was used as the main proton transfer medium. Its molecular structure contains phosphoric acid groups which are directly linked to carbon atoms and may also contain-OH, -CH_2, -COOH and other groups. There are C-P bonds in the molecular structure, and this bond is much stronger than the C-O-P bond. Composite membranes obtained in this way possess more remarkable chemical stability and high temperature resistance. The content of its high phosphate group indicates that it can be used as proton conductor in polymer membrane. Glutaraldehyde was used as a crosslinking agent, and PBTCA was doped into PVA matrix by solution casting technique. The phosphate group was immobilized by the esterification between -COOH on PBTCA and -OH on PVA. At the same time, sulfonated succinic acid (SSA), which is a typical sulfonated reagent, was selected as a proton transfer media to prepare sulfonated proton exchange membrane. FTIR, XRD, TGA and AC Impedance were operated to explore the different structure and properties of two composite membrane. It is hoped that the proton conducting membranes with high proton conductivity, favorable methanol barrier ability and low cost can be obtained through phosphonated polymers.

Experimental section

Materials

Fully hydrolyzed poly(vinyl alcohol) (PVA, a polymerization degree of 2400) was supplied by Sichuan vinylon factory of Sinopec (Chongqing, China). Sulfosuccinic acid (SSA, 70 wt.% solution in water) were purchased from Sigma-Aldrich Co. and 2-phosphonobutane-1,2,4-tricarboxylic acid (PBTCA) were purchased from Shandong Taihe water treatment technology co., LTD (Shandong, China). Methanol (MeOH) was analytical grade from Aldrich Co. and the distilled water was used in this study.

Preparation of PVA proton exchange membranes

PVA–PBTCA membranes were fabricated by solution casting technique. To be specific, 30 mL of 5 wt% PVA aqueous solution was prepared by dissolving required amount of PVA in water at 363 K followed by its stirring in order to make it dissolved completely until a homogeneous PVA solution was obtained. Then the obtained solution was doped with SSA and PBTCA in proportion respectively and continue to stir for 1 h to mix well followed by its cooling to indoor temperature (~298 K). The resulting solution was casted into a membrane on a polyfluortetraethylene plate and then dried in an oven at 50 °C to obtain a dry membrane followed by its further heat treatment under 100 °C for complete reaction [18]. The reaction process of PBTCA, SSA and PVA is shown in Fig. 1.

For simplicity, the obtained PVA complex membranes with different amounts of proton transfer medium are denoted as PVA-X-Y, where X represents the mass percentage of the added proton transfer medium and PVA, and Y represents SSA or PBTCA.

Experimental operation process is shown in Fig. 2.

Characterizations

Fourier transform infrared spectroscopy (FT-IR)

The infrared spectrum of the membranes were recorded on a Nicolet iS50 Fourier infrared tester (Nicolet, USA) through the Fourier attenuation total reflection method with a wave number of 500~4000 cm^{-1}. Before the test, the composite membranes were dried in a 50 °C oven to reduce the influence of residual moisture in the specimen on the infrared spectrum.

X-ray diffractometer(XRD)

The crystallization state of proton exchange membranes was analyzed on an X-ray diffractometer (tall Ultima IV, Rigaku Japanese company) at a voltage of 40 kV and a tube current of 40 ma, and scanning speed is 10 ° / min. The proton exchange membrane need to be dried in 50 °C oven before the test. The dried proton exchange membrane sample was cut into appropriate size, and then glued to the glass sample frame by tapes for following testing.

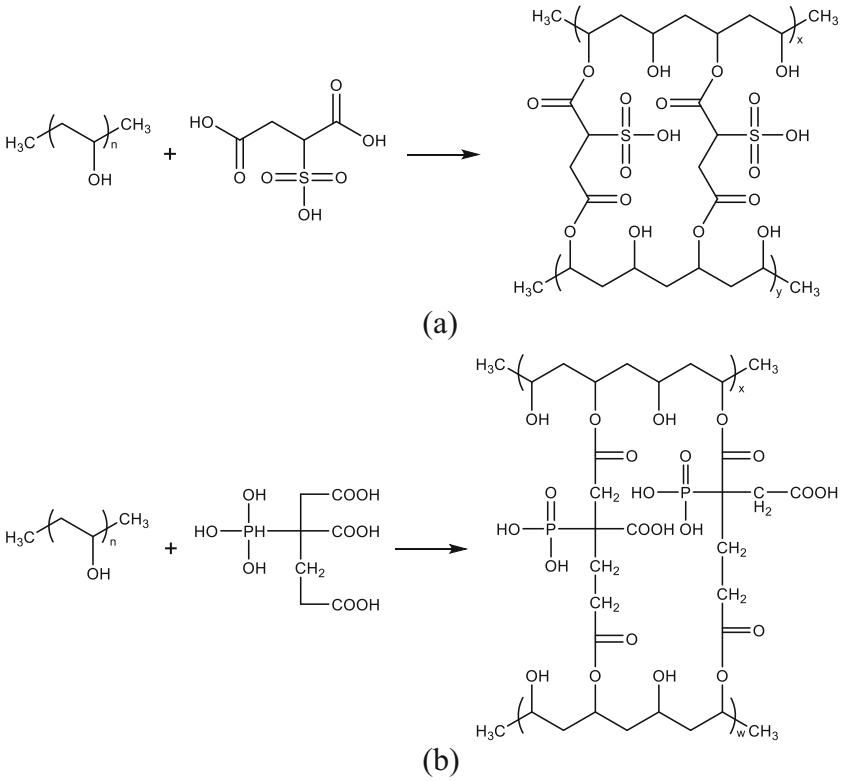

Fig. 1 Possible reaction mechanism of PVA with SSA (**a**) and PBTCA (**b**)

Thermogravimetric analysis(TGA)

The thermal stability of the membranes was studied on a Synchronized TG209F1 type thermal analyzer (Germany Netzsch companies) at a temperature range of 30 ~ 600 °C and a heating rate of 10 °C/min in a nitrogen atmosphere. Before the test, membrane samples should be dried in a vacuum oven at 50 °C for 2 h.

Testing mechanical properties

The mechanical properties of the membranes were measured by CMT6104 microcomputer controlled electronic universal testing machine (MTS) with a test speed of 10 mm/min at room temperature (25 °C). The sample membrane was cut into small splines of 40 mm × 10 mm in size, and the digital display spiral micrometer instrument was used to measure the average thickness of samples. The tensile strength and elongation at break of the membranes were finally obtained through stress-strain curves. Five samples were tested for each sample, and their average value was taken as the final data.

Swelling degree

The dimensional stability of the membranes was characterized by the swelling degree. The membrane was cut into a regular shape, and then immersed in a beaker containing deionized water for 24 h at room temperature (25 °C). After sufficiently swollen with deionized water, the membranes were taken out and wiped with a filter paper. The length and the width of the

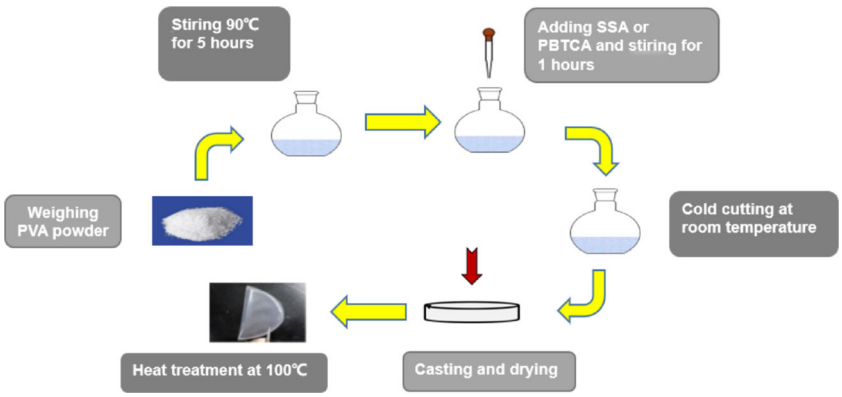

Fig. 2 Flow chart of experimental operation

membranes were immediately measure and the area of the membranes was marked as A_w. Then the membrane was dried in a blast drying oven at 50 °C until its weight did not change. The length and width of the dried membrane were recorded and the area of the dried membrane was marked as A_d. [19] The swelling degree of the membrane can be characterized by the percentage of the change in the area of the membranes were calculated by the eq. (1):

$$Swelling\ degree\ (\%) = \frac{A_w - A_d}{A_d} * 100\% \quad (1)$$

Proton conductivity testing

The membrane was placed in two stainless steel electrodes to form a blocking electrode. The resistance of the membranes was measured by AC impedance method using the CHI600E electrochemical workstation (Shanghai Chenhua Instrument co. LTD, China) at a scanning frequency range of 0.1–106 Hz and a voltage amplitude of 5 mV at room temperature. The proton conductivity of the membranes was calculated according to the resistance obtained by the test, as shown in the following formula (2):

$$\sigma = \frac{L}{AR} \quad (2)$$

where σ is the proton conductivity (S/cm); L is the thickness of the membrane (cm); A is the effective contact area of the membrane during the test (cm^2); R is the resistance of the membrane sample (Ω).

The membrane sample was cut into a circle with a diameter of 2 cm, and then soaked in water for 24 h until fully absorbed. The thickness of the membrane was measured by a digital spiral micrometer. Resistance R was obtained from the ac impedance spectra (Fig. 3) measured by the electrochemical workstation. In the ac impedance spectrum, the value corresponding to the intersection point of the line and the x-coordinate is the measured resistance value R of the membrane, as shown in Fig. 3. Above operation was repeated for three times [6].

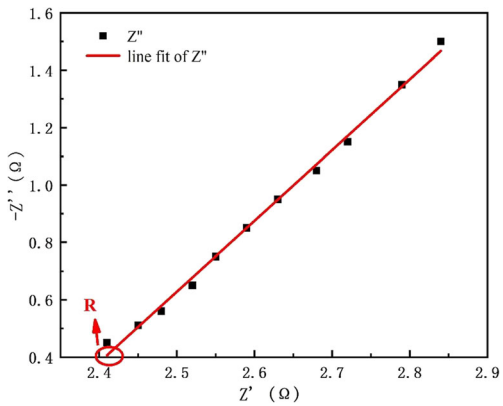

Fig. 3 Typical impedance plot of the membrane sample

Using the same test device, the membrane was cut into a circle with a diameter of 2 cm. The membrane was allowed to place in the air at room temperature for 24 h to achieve the in-membrane humidity balance and the indoor humidity was kept at 50%. The proton conductivity at 50%RH at room temperature was measured by the same test method.

Methanol permeability test

The methanol permeability was measured via a self-made diaphragm diffusion cell. As shown in Fig. 4, the diaphragm diffusion cell consists of two identical glass chambers with an inner diameter of approximately 19 mm and a volume of approximately 250 ml. The membrane was made into a square sample with size of 2×2 cm^2 before testing and soaked in deionized water for 24 h to allow it to fully absorb water. The surface water was removed by a filter paper, and the thickness of the membrane was measured with a Digital display screw micrometer. Then the resultant membrane was sandwiched between two rubber sealing gaskets followed by its fixation between the two glass chambers. At the same time, 250 mL of deionized water was added to Room B, and 250 mL of 2 M aqueous methanol solution was added to Room A. Turn on the magnetic stirrer, and start timing. 1 mL sample was taken from the A half chamber with a pipette every 30 min, and 4 points were taken for each membrane to be tested. The concentration of the sample was measured with a gas chromatograph (Agilent 7820A). The time was chosen as the abscissa and the methanol concentration in the A half chamber was chosen as the ordinate. In this way, the curve of methanol concentration over time was obtained, and the slope S was calculated by straight line fitting.

According to the principle of dissolution-diffusion, the transport process of methanol molecules in the proton exchange membrane can be divided into three steps: the adsorption process on the anode side of the membrane, the diffusion process in the membrane under the action of concentration difference and chemical gradient, and the desorption process on the cathode side of the membrane. It is assumed that the penetration process conformed to Fick law, and the concentration of methanol on the left feed side marked as C_A was much

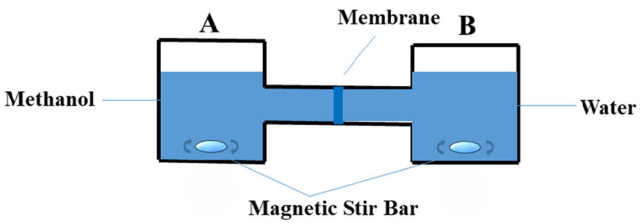

Fig. 4 The schematic depictions of testing facility for methanol permeability measurement

higher than that on the right marked as C_B, so the relationship between the concentration of the methanol and time is as shown in eq. (3) [20]:

$$C_B(t) = \frac{AD_K}{V_B L} C_A(t - t_0) \quad (3)$$

where D is the diffusion coefficient of methanol set to a constant, and K is the partition coefficient independent of the concentration. D_K is the permeability P of methanol, and t_0 is the lag time, so the methanol permeability of the membrane (Methanol permeability, P, $cm^2 \cdot s^{-1}$) can be expressed as:

$$P = \frac{S\, V_B\, L}{A\, C_A} \quad (4)$$

where S is the linear fitting slope of the curve of methanol concentration over time in the B half chamber; V_B is the volume of the solution in the cell B, 30 mL; L is the thickness of the membrane (cm); A is the effective area of the membrane (cm^2); C_A is the initial concentration of methanol in the cell A, 2 $mol \cdot L^{-1}$.

Results and discussion

FTIR analysis of PVA composite membrane

The infrared spectrums of the pure PVA membrane, the PVA-PBTCA-33 membrane and the PVA-SSA-33 membrane were shown in Fig. 5. It can be seen that 915 cm^{-1} and 1005 cm^{-1} are P-OH stretching vibration absorption peaks. Moreover, the absorption bands at 1030 and 1140 cm^{-1} indicate the presence of sulfonic acid group by the introduction of SSA. The C=O absorption peak of the ester bond-COO- at 1710 cm^{-1} and the C-O-C asymmetric absorption peak at 1205 cm^{-1} indicate that both SSA and PBTCA are successfully grafted onto the PVA backbone by the esterification between –OH in PVA and –COOH in SSA and PBTCA.

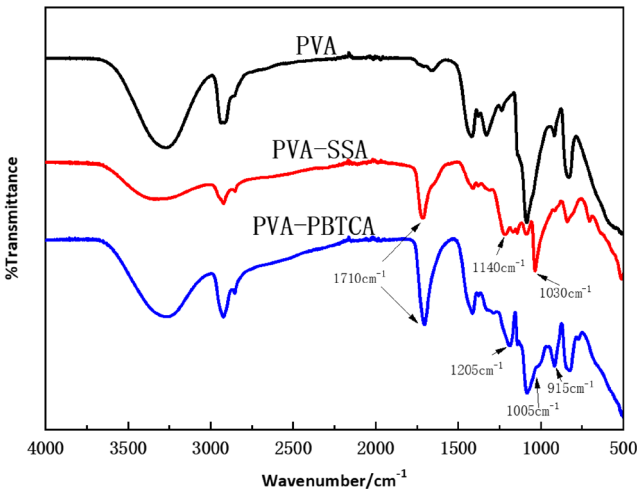

Fig. 5 FTIR spectra of pure PVA, PVA-33-SSA and PVA-33-PBTCA membranes

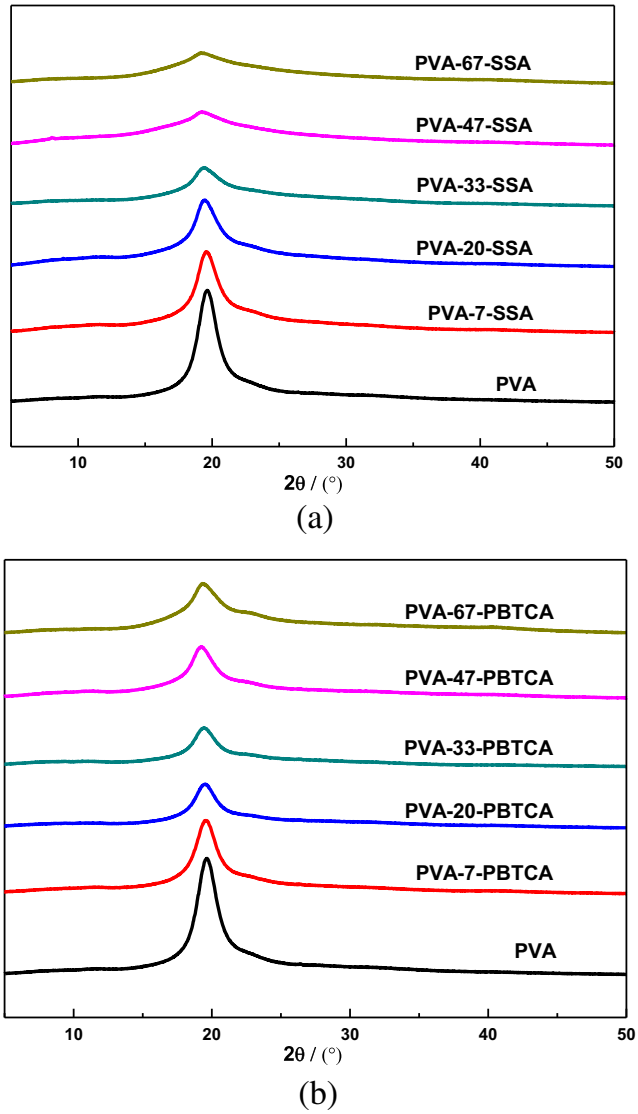

Fig. 6 XRD spectra of pure PVA and PVA-SSA (**a**) and PVA-PBTCA (**b**) membranes with different content

XRD measurements

Figure 6 shows the X-ray diffraction pattern of pure PVA membrane, PVA-SSA membranes and PVA-PBTCA

Table 1 The degree of crystallinity of PVA-SSA membranes with different content

Membrane	degree of crystallinity
PVA	55.32%
PVA-7-SSA	50.98%
PVA-20-SSA	41.33%
PVA-33-SSA	30.79%
PVA-47-SSA	21.67%
PVA-67-SSA	13.45%

Table 2 The degree of crystallinity of PVA-PBTCA membranes with different content

Membrane	degree of crystallinity
PVA-7-PBTCA	44.77%
PVA-20-PBTCA	39.52%
PVA-33- PBTCA	35.14%
PVA-47- PBTCA	31.26%
PVA-67- PBTCA	24.55%

membranes, respectively. It can be seen that the strong crystallization peak appearing at $2\theta = 19.8°$ is the characteristic diffraction peak of PVA. With the increase of the SSA and PBTCA contents, the diffraction peak of PVA-SSA membranes and PVA-PBTCA membranes shows a similar change trend that the shape of the peak gradually widens and the intensity of the peak gradually decreases. The degree of crystallinity of PVA-SSA and PVA-PBTCA membranes with different content is listed in Table 1 and Table 2, respectively. It can be seen that the crystallinity of two membranes gradually decreases with the increase of SSA and PBTCA content. This is because that the addition of PBTCA and SSA destroys the ordered structure of PVA molecule by esterification reaction with the hydroxyl group in the main chain. The intermolecular interaction between the PVA molecules after esterification decreases. The molecular spacing and free volume also increase. Comparing Fig. 6(a) and (b), it is found that the intensity of diffraction peak of PVA-PBTCA membrane is larger than that of PVA-SSA membrane. This is because PBTCA is less acidic than SSA, and the catalysis of PBTCA on esterification reaction with PVA is weaker than that of SSA. The degree of esterification of PBTCA and PVA is relatively low, and the less hydrogen bond in PVA is damaged. As the content of PBTCA increases, the content of phosphate groups increases, and a dynamic hydrogen bond network can be formed in the membrane. It is advantageous for stabilizing the crystal structure, and thus the degree of crystallinity is higher than the PVA-SSA membrane when the PBTCA content is 67%.

TGA analysis

Figure 7 shows the thermogravimetric curves of pure PVA membrane, PVA-SSA and PVA-PBTCA membranes with different content of SSA and PBTCA. It can be seen from the figure that the pure PVA membrane has better thermal stability, while the first stage of its thermal weight loss is between 80 °C and 120 °C. Because of the water-absorbing quality of the hydroxyl group, the first weightless platform is mainly caused by the evaporation of water in the PVA membrane. The second stage of thermal weight loss occurs between 280 °C and 400 °C, mainly due to the loss of mass caused by the degradation of the hydroxyl group on the main chain. The third stage of thermal weight loss occurs above 400 °C, it is the degradation of the backbone of PVA molecular.

Compared with the PVA membrane, the thermal stability of PVA-SSA membranes and PVA-PBTCA membranes after esterification and cross-linking is reduced. This is because the esterification reaction destroys the hydrogen bonding of PVA, which gives rise to the decline of crystallinity and thermal stability. The weight loss process of PVA-SSA membrane is divided into three stages. The first stage is between 100 °C and 160 v, and the mass loss of the membrane is about 30%, which corresponds to the by-product water produced from the further esterification in PVA-SSA membrane and bound water in the membrane. The second stage is between 180 °C and 260 °C, where the mass loss of the membrane increases from 5 to 20% with the increase of SSA content, corresponding to the fracture of the sulfonic acid group and ester bond in the PVA-SSA membrane. The third stage is above 400 °C, which represents the degradation of the PVA molecular backbone.

The weight loss process of PVA-PBTCA membrane is also divided into three stages, which is similar to that of PVA-SSA membrane. The first stage is between 100 °C and 150 °C, which is mainly the evaporation of the bound water and he by-product water produced from the further esterification in the membrane. The second stage is between 190 °C and 330 °C, where the dehydration condensation reaction of the partial hydroxy between the phosphoric acid groups and the fracture of the ester group occur. The higher the content of PBTCA is, the greater the damage to the hydrogen bonds of

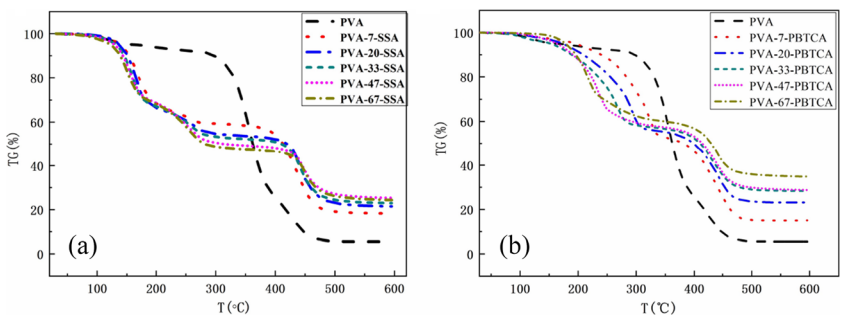

Fig. 7 Thermogravimetric analysis of PVA, PVA-SSAc (**a**) and PVA-PBTCA (**b**) membranes

PVA is. Meanwhile, the more the crystallinity of the membrane decreases, the lower the thermal decomposition temperature of the membrane is. The third phase is between 370 °C and 600 °C, which is the degradation of the PVA polymer molecular backbone. By comparing the TG curves of the two membranes, it can be found that the thermal decomposition temperature of the PVA-PBTCA membrane in the second weight loss phase is higher than that of the PVA-SSA membrane. This is because of the presence of the phosphate group, making the PVA-PBTCA membrane easy to form hydrogen bond structure. On the other hand, PVA-PBTCA membranes can maintain more than 95% of the components below 150 °C. PVA-PBTCA membrane has the higher crystallinity and the thermal stability of PVA-PBTCA membrane is better than that of PVA-SSA membrane.

Swelling degree

It is well known that membranes based on sulfonated polymers rely critically on water for the proton conductivity. Good water absorption of the membrane can guarantee a certain proton conductivity, and its good dimensional stability is also a prerequisite for ensuring the use of the membrane. The swelling degree of the membrane is generally used to characterize the dimensional stability of the membrane. The swelling degree of the membrane at room temperature is shown in Fig. 8. It can be seen from the figure that when the amount of SSA and PBTCA is increasing, the swelling degree of the PVA-SSA and PVA-PBTCA membranes gradually decreases. The increase of SSA and PBTCA content enhances the interaction between the sulfonic acid group and the phosphonic acid group with the hydroxyl group of PVA, and destroys hydrogen bond network in the PVA membrane. As a result, the crystallinity of the PVA-SSA and PVA-PBTCA membranes decreases and the swelling degree of the membranes

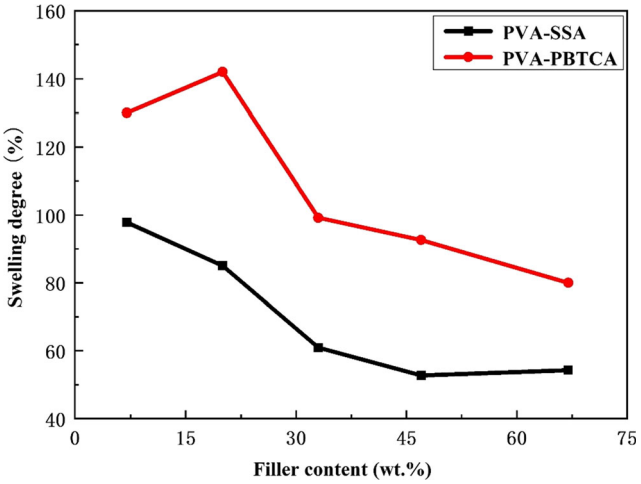

Fig. 8 The change of swelling degree in the PVA-SSA and PVA-PBTCA membranes depending on the content of SSA and PBTCA

increases. At the same time, it is found that the crosslinking degree of the membranes gradually increases with the further increase of the SSA and PBTCA content, as shown in Table 3 and Table 4. This is mainly due to the increase of esterification reaction and the cross-linking structure in the membrane. The increase of crosslinking degree of the membranes will limits the movement of the PVA molecular chain. Therefore, the anti-swelling property of the membrane is enhanced and the dimensional stability is improved.

Mechanical properties of PVA-PBTCA and PVA-SSA membranes

The mechanical properties of PVA-PBTCA and PVA-SSA membranes were shown in Figs. 9 and 10, respectively. It can be seen from Fig. 9 that compared with the pure PVA membrane, the addition of SSA causes the decrease the tensile strength of the PVA-SSA membranes and the increase of the elongation at break. Moreover, with the increase of the SSA content, the tensile strength decreases first and then increases, and the elongation at break gradually decreases. This is because the addition of SSA destroys the hydrogen-bond interaction in the PVA molecular chain, which reduces the crystallinity and tensile strength in the membrane. With the content of SSA further increase, the degree of esterification and the cross-linked structure increase, which leading to the improvement of the tensile strength. On the other hand, the increase of the cross-linked structure in the membrane weakens the motion activity of molecular chain, therefore the elongation at break of the membrane is further reduced.

Figure 10 is the stress-strain curves of PVA-PBTCA membranes with different amounts of PBTCA. As shown in Fig. 10, the increase of PBTCA content also causes the decrease in the tensile strength of the PVA-PBTCA membranes. With the increase of the content of PBTCA, the tensile strength of the PVA membranes decreases first and then increases, and the elongation at break gradually decreases. Similar to the PVA-SSA membrane, the addition of PBTCA destroys the intermolecular forces in the PVA membranes, resulting in the decrease of crystallinity and tensile strength. As the content of PBTCA continues to increase, the cross-linked structure of the membrane increases, and the tensile strength of the membrane also increases. However, the tensile

Table 3 The degree of crosslinking of PVA-SSA membranes with different content

Membrane	Degree of crosslinking
PVA-7-SSA	6%
PVA-20-SSA	15%
PVA-33-SSA	30%
PVA-47-SSA	33%
PVA-67-SSA	39%

Table 4 The degree of crosslinking of PVA-PBTCA membranes with different content

Membrane	Degree of crosslinking
PVA-7-PBTCA	8%
PVA-20- PBTCA	14%
PVA-33- PBTCA	35%
PVA-47- PBTCA	40%
PVA-67- PBTCA	44%

strength of the PVA-PBTCA membrane is larger than that of the PVA-SSA membrane, and the elongation at break of the PVA-PBTCA membrane is smaller than that of the PVA-SSA membrane. This is because the acidity of PBTCA is weaker than that of SSA, and the catalytic effect on the esterification reaction with PVA is less than that of SSA. Therefore, the damage of PBTCA to hydrogen bond of PVA molecules is smaller. When the PBTCA increases, the content of phosphate groups also increases, which is favorable to the formation of hydrogen bond network in the PVA-PBTCA membrane. At the same time, the increase of hydrogen bond can enhance the strength of the membrane, the PVA-PBTCA membrane increases.

Proton conductivity

The vertical conductivity of the membrane was tested by AC impedance method. The conductivity of pure PVA membrane is 0.4×10^{-4} S/cm, which is far less than that of PVA-SSA and PVA-PBTCA membranes. This is because pure PVA does not contain any ion exchange group, and it needs to be added other proton conductors to obtain the ideal conductivity. It can be seen from Fig. 11 that as the content of the proton transfer medium increases, the proton conductivity of PVA-SSA

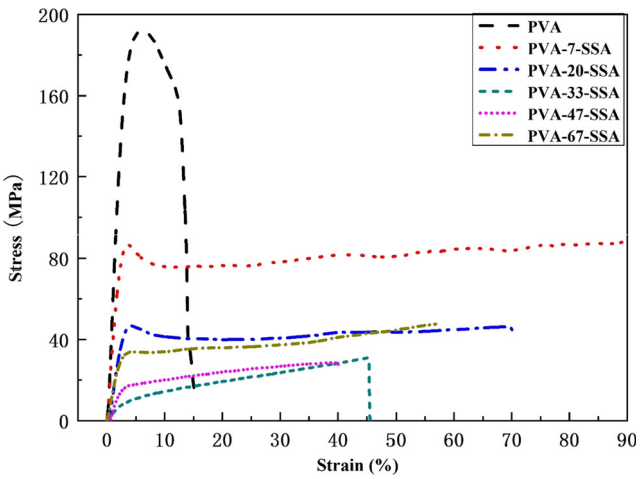

Fig. 9 Stress-strain curves of PVA and PVA-SSA membranes with different SSA content

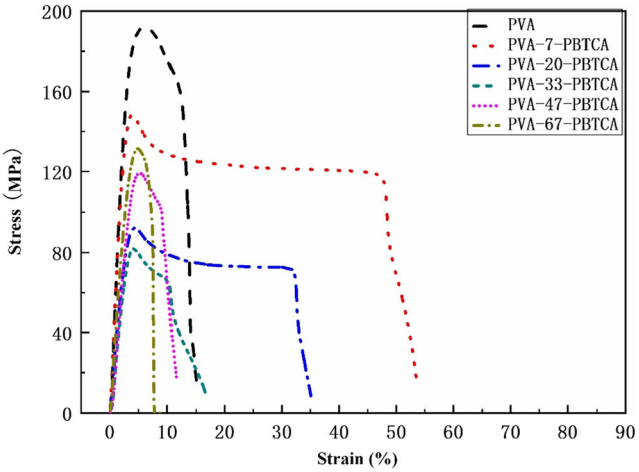

Fig. 10 Stress-strain curves of PVA and PVA-PBTCA membranes with different PBTCA content

membrane and PVA-PBTCA membrane gradually increase. To be specific, when the content of proton transfer medium is 33%, the proton conductivity of the two above-mentioned membranes reaches their highest value, which is 1.51×10^{-3} S·cm^{-1} and 1.3×10^{-3} S·cm^{-1}, respectively. When the content of SSA and PBTCA content is relatively low, there is less esterification in the membrane. Therefore, the cross-linking density of the membrane is low and the free volume is large. At the same time, the increase in water absorption rate of the membrane is conducive to the transfer of protons between water molecules and proton transfer sites. Because the -SO_3H group has stronger proton dissociation capacity when the hydration degree of the membrane is higher, the conductivity of PVA-SSA membrane is higher than that of PVA-PBTCA membrane when the content of SSA and PBTCA content is relatively low. On the other hand, when the content of SSA increased further, the number of ester bonds and the degree of crosslinking of the membrane increased. The water absorption and swelling degree decreased, and the motion of molecular chain was limited, so the conductivity of PVA-SSA membranes began to decline.

When the content of PBTCA further increase, the degree of crosslinking of the PVA-PBTCA membrane increases, and the water absorption and swelling degree in the membrane decreased, leading to the decline of the proton conductivity of the membrane to some extent. Due to the amphoteric characteristic of -PO_3H_2, a dynamic hydrogen bond network can be fabricated in the membrane, which facilitated the transfer of protons along hydrogen bonds in the membrane. Therefore, the proton conductivity of PVA-PBTCA membrane decreased less than that of PVA-SSA membrane.

To further investigate the effect of sulfonic acid groups and phosphate groups on the proton conductivity of the membranes, the proton conductivity of the PVA-SSA membrane and the PVA-PBTCA membrane were tested at low humidity. The indoor relative humidity was kept at about 50%, and the

membranes were placed in the air at room temperature for 24 h to achieve humidity balance inside the membrane. The proton conductivity of PVA-SSA membrane and PVA-PBTCA membrane were tested by the same method, and the corresponding results were shown in Fig. 12. It can be seen from the figure that at room temperature and low humidity, the proton conductivity of the membrane changed slightly with the increase of the content SSA and PBTCA. The PVA-PBTCA membrane has a higher proton conductivity of 8.17×10^{-5} S/cm while the proton conductivity of PVA-SSA membrane reaches a peak only at 4.09×10^{-5} S/cm, which is lower than that of the PVA-PBTCA membrane. This is because, under the condition of low humidity, the proton transfer process is dominated by the "jumping mechanism". [22] In this way, protons are transported jumping from one proton transfer site to another. The sulfonic acid group has weaker binding ability to protons, and the proton transport cannot be completed efficiently. However, the phosphate group can be used as both a proton donor and a proton acceptor, making it easy to form a dynamic hydrogen bond network in the PVA-PBTCA membrane, which is conducive to proton transfer. On the other hand, the free energy barrier for transferring protons between phosphate groups is lower, and the transfer of protons is easier. Therefore, the proton conductivity of PVA-PBTCA membrane at room temperature and 50% RH is higher than that of PVA-SSA membrane.

Methanol permeability

The methanol permeability of the membrane is also an extremely important parameter for proton exchange membrane fuel cells, especially direct methanol fuel cells. Figure 13 shows that methanol permeability of the different PVA membranes at room temperature. It can be seen that when the content of SSA and PBTCA is 7%, the methanol permeability of PVA-SSA membrane and PVA-PBTCA membrane respectively were 1.21×10^{-6} $cm^2 \cdot s^{-1}$ and 1.32×10^{-6} $cm^2 \cdot s^{-1}$, which was higher than that of nafion-117 membrane tested under the same conditions. When the content of SSA and PBTCA increased gradually, the cross-linking structure in the membrane increased and the water absorption rate decreased. Therefore, the methanol permeability of the membranes also decreased. When the content of SSA and PBTCA was 67%, the methanol permeability of PVA-SSA membrane and PVA-PBTCA membrane were 0.82×10^{-6} $cm^2 \cdot s^{-1}$ and 0.94×10^{-6} $cm^2 \cdot s^{-1}$. The methanol transmittance of pure PVA is very low. When the content of SSA and PBTCA reaches 67%, the methanol permeability of the membrane is close to the pure PVA membrane.

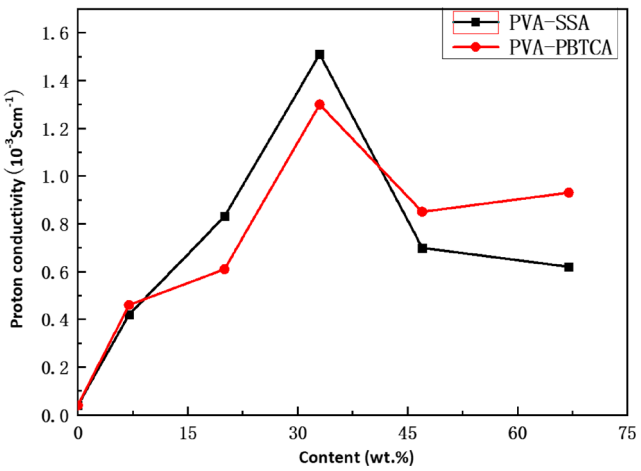

Fig. 11 Proton conductivity with different content for PVA-SSA and PVA-PBTCA membranes

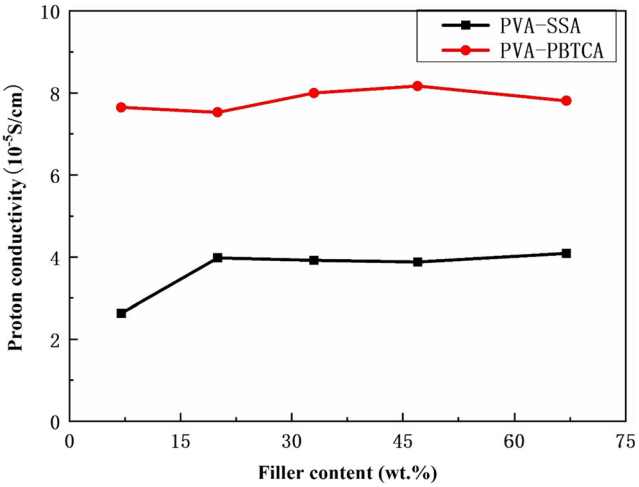

Fig. 12 Proton conductivity with different content for dried PVA-SSA and PVA-PBTCA membranes content

Conclusion

In the present work, PBTCA and SSA were used as a proton source and a cross-linking agent to prepare the crosslinked

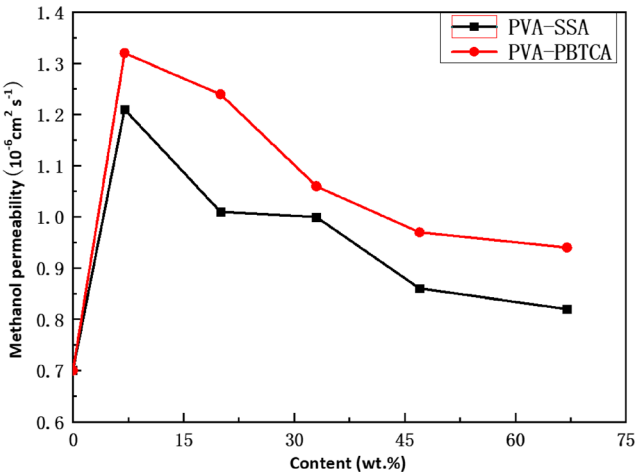

Fig. 13 Methanol permeability of the membranes at room temperature

PVA membranes for a potential polymer electrolyte membrane in fuel cell applications. The -COOH of the proton transfer medium is esterified with the -OH of PVA to form a cross-linked structure. The TGA curve shows that the thermal stability of the PVA-PBTCA phosphorylated proton exchange membrane is better than that of the PVA-SSA sulfonated proton exchange membrane, indicating that the phosphate group is superior to the sulfonic acid group in terms of the thermal stability. When the content of SSA and PBTCA is 33%, PVA-SSA membrane and PVA-PBTCA membrane with the highest proton conductivity were 1.51×10^{-3} S·cm^{-1} and 1.3×10^{-3} S·cm^{-1}, respectively. Under the condition of low humidity, the PVA-PBTCA membrane has a proton conductivity of 8.17×10^{-5} S·cm^{-1}, which is twice than that of the PVA-SSA membrane, indicating that phosphated proton exchange membrane is not very dependent on the water content for proton transfer and can be used under high temperature and low humidity. The methanol permeability of the membrane decreased with the increase of the content of SSA and PBTCA. When the content of SSA and PBTCA was 67%, the methanol permeability is 0.82×10^{-6} cm^2·s^{-1} and 0.94×10^{-6} cm^2·s^{-1}, which was lower than that of Nafion-117 membrane.

Acknowledgments This work was supported by the National Natural Science Foundation of China (NSFC 51503134, 51721091) and the State Key Laboratory of Polymer Materials Engineering (Grant 679 No. SKLPME 2017-3-02).

References

1. Jacobson MZ, Colella WG, Golden DM (2005) Cleaning the air and improving health with hydrogen fuel-cell vehicles. Science 308(5730):1901–1905
2. Steele BCH, Heinzel A (2001) Materials for fuel-cell technologies. Nature 414(6861):345–352
3. Jung WS (2018) Study on durability of Pt supported on graphitized carbon under simulated start-up/shut-down conditions for polymer electrolyte membrane fuel cells. J Energy Chem 27(1):326–334
4. Sun X, Xu H, Zhu Q, Lu L, Zhao H (2015) Synthesis of Nafion®-stabilized Pt nanoparticles to improve the durability of proton exchange membrane fuel cell. J Energy Chem 24(3):359–365
5. Zhang H, Shen PK (2012) Recent development of polymer electrolyte membranes for fuel cells. Chem Rev 112(5):2780–2832
6. Carretta N, Tricoli V, Picchioni F (2000) Ionomeric membranes based on partially sulfonated poly(styrene): synthesis, proton conduction and methanol permeation. J Membr Sci 166(2):189–197
7. Lufrano F, Baglio V, Staiti P, Antonucci V, Arico' AS (2013) Performance analysis of polymer electrolyte membranes for direct methanol fuel cells. J Power Sources 243:519–534
8. DELUCA N, ELABD Y (2006) Nafion®/poly(vinyl alcohol) blends: effect of composition and annealing temperature on transport properties. J Membr Sci 282(1–2):217–224
9. Chang Y, Wang E, Shin G, Han J, Mather PT (2007) Poly(vinyl alcohol) (PVA)/sulfonated polyhedral oligosilsesquioxane (sPOSS) hybrid membranes for direct methanol fuel cell applications. Polym Adv Technol 18(7):535–543
10. Paddison SJ (2003) Proton conduction mechanisms at low degrees of hydration in sulfonic acid–based polymer electrolyte membranes. Annu Rev Mater Res 33(1):289–319
11. Schuster M, Rager T, Noda A, Kreuer KD, Maier J (2005) About the choice of the Protogenic group in PEM separator materials for intermediate temperature, low humidity operation: a critical comparison of sulfonic acid, Phosphonic acid and imidazole functionalized model compounds. Fuel Cells 5(3):355–365
12. Mehta V, Cooper JS (2003) Review and analysis of PEM fuel cell design and manufacturing. J Power Sources 114(1):32–53
13. Li Z, He G, Zhang B, Cao Y, Wu H, Jiang Z, Tiantian Z (2014) Enhanced proton conductivity of Nafion hybrid membrane under different Humidities by incorporating metal–organic frameworks with high Phytic acid loading. ACS Appl Mater Interfaces 6(12): 9799–9807
14. Allcock H (2002) Phenyl phosphonic acid functionalized poly[aryloxyphosphazenes] as proton-conducting membranes for direct methanol fuel cells. J Membr Sci 201(1–2):47–54
15. Kannan R, Islam MN, Rathod D, Vijay M, Kharul UK, Ghosh PC, Vijayamohanan K (2008) A 27-3 fractional factorial optimization of polybenzimidazole based membrane electrode assemblies for H2/O2 fuel cells. J Appl Electrochem 38(5):583–590
16. Jin Y, Diniz Da Costa JC, Lu GQ (2007) Proton conductive composite membrane of phosphosilicate and polyvinyl alcohol. Solid State Ionics 178(13–14):937–942
17. KIM D (2004) Preparation and characterization of crosslinked PVA/SiO2 hybrid membranes containing sulfonic acid groups for direct methanol fuel cell applications. J Membr Sci 240(1–2):37–48
18. Gu S, He G, Wu X, Guo Y, Liu H, Peng L, Xiao G (2008) Preparation and characteristics of crosslinked sulfonated poly(phthalazinone ether sulfone ketone) with poly(vinyl alcohol) for proton exchange membrane. J Membr Sci 312(1–2):48–58
19. Cahan BD (1993) AC impedance investigations of proton conduction in Nafion™. J Electrochem Soc 140(12):L185
20. Pivovar BS, Wang Y, Cussler EL (1999) Pervaporation membranes in direct methanol fuel cells. J Membr Sci 154(2):155–162